The right way to ride the wrong bike: An exploration of Klein's 'unridable' bicycle

B.D. Coller[1*]

1 Department of Mechanical Engineering, Northern Illinois University, DeKalb, Illinois, USA

* bcoller@niu.edu

Abstract

Professor Richard Klein and his students built a bicycle with a rather interesting feature: no one was able to ride it. A prize was offered. Hundreds of students and cycling enthusiasts attempted it. Years passed, and the prize money grew. This article is an exploration of the dynamics and control of the unridable bicycle from the perspective of an engineer determined to ride it. By developing simple models of a bicycle as an inverted pendulum attached to a wheeled carriage that provides steer kinematics, one can pinpoint a physical mechanism which explains why the rear-steered configuration is difficult to balance. By applying a state space control perspective, one can illuminate limitations and opportunities for stabilization. The end result is that Klein's unridable bicycle is ridable, with the right strategy and ample practice.

Introduction & Background

In 1986, Richard Klein and his students made an unusual modification to a rather normal bicycle [1]. A photograph of the bicycle is shown in Fig 1 They placed the handlebar where the seat normally goes and moved the seat to where the handlebar normally belongs. They also moved the chain ring and wheel drive sprocket to the other side of the bike. Therefore, when a rider sits on the seat, places their hands on the handlebar in front of them, and begins pedaling, the bicycle begins moving in the direction that the rider is facing, as expected. What makes the bicycle different is that the wheel which steers is the rear wheel. The non-steered wheel, which is now at the front of the bicycle, is mechanically connected to the pedals via drive chain. Klein gave a name to this bike: Rear-Steered Bike I (RSB1).

For this bicycle, the handlebar and fork are separated from each other and placed at opposite ends of the bike as shown in the photo of Fig 1. The two parts are connected to each other mechanically via the steer chain wrapped around two steer sprockets of equal diameter. If the steer chain is wrapped in a simple loop configuration as shown in Fig 2A, then a left turn of the handlebar by

Fig 1. Klein's "unridable bicycle." A photograph of the rear-steered bicycle that Richard Klein and others deemed unridable.

angle δ causes the fork and the steered wheel to rotate the same angle δ and in the same direction. However, since the steered wheel is at the rear of the bicycle, such a leftward turn of the handlebar causes the entire bike to turn to the right.

Another way to configure the steer chain is shown in Fig 2B. Here, the chain makes a figure-8 shaped loop. As a result, the fork turns in opposite direction as the handlebar. In this case, the bicycle turns in the same direction that the handlebar is rotated. Either configuration is possible on Rear-Steered Bike I (RSB1).

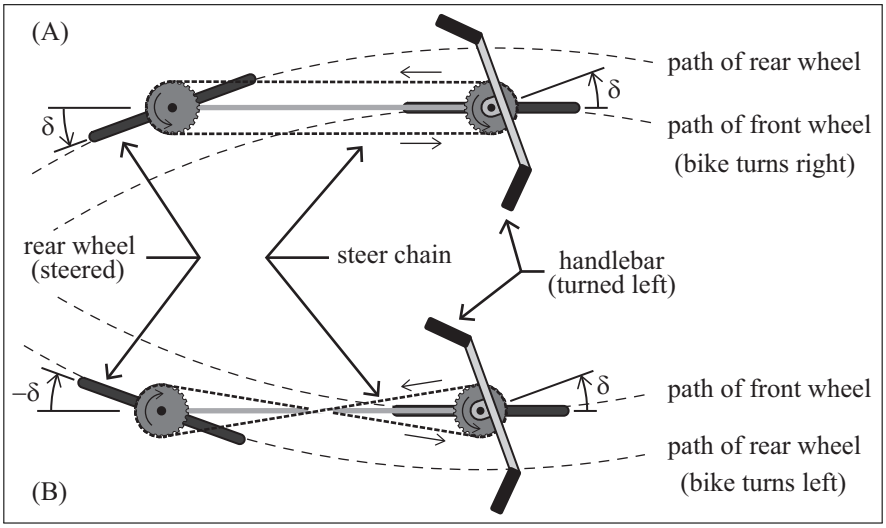

Fig 2. Steer chain configuration." A: When the steer chair wraps around the sprockets in a simple loop, a leftward turn of the handlebar causes the rear-steered bicycle to execute a rightward turn. B: When the steer chain is in a figure 8 configuration, the bicycle turns in the same direction that the handlebar is turned.

Regardless of which way the steer chain is configured, the simple act of making the rear wheel the one that steers, makes the bike have really odd

behavior. In the Supporting Information section at the end of this article, there are links to several videos. The first, S1 Video shows mechanical engineering students attempting to ride Klein's Rear-Steered Bike I. To be fair the video shows students' first interactions with the bike. However, it typically does not get much better after spending hours trying to wrap their minds around it.

A "Backward Brain Bicycle"

It is well known that the simple act of switching the sign of the input/output relationship, so that a bike turns in the opposite direction that the handlebar is steered, is sufficient to make the task of balancing a bicycle upright exceedingly difficult. The popular YouTube channel, *Smarter Every Day*, has an episode devoted to this specific topic [2] in which Destin Sandlin added a geared connection between the handlebar and fork of a normal front-steered bicycle. When the rider would turn the handlebar one way, the fork would turn the front wheel by the same angle about its steer axis, but the opposite direction.

To be clear, Sandlin and co-workers did nothing else to modify the dynamics of their "Backwards Brain Bicycle." In principle, it should be just as easy to stabilize. The rider would just need to respond with the opposite steer input in response to a perceived amount of bicycle lean. However, at least in Sandlin's case, it took nearly a month of daily dedicated training to de-program the subconscious part of the brain that holds those automatic responses and replace those responses with ones that produce the opposite handlebar motion.

The story of the "Backward Brain Bicycle" is relevant here because of the important difference between it and Klein's "Rear-Steered Bike I" (RSB1). As presented in this article, *the dynamics of the rear-steered bicycle are fundamentally different than those of the front-steered counterpart.* While there might be some long-term training required to ride a bike similar to RSB1, the strategies may be fundamentally different. To ride the flipped bike might require different levels of precision, athleticism, and/or cognitive engagement in the riding process.

Klein's Challenge

Richard Klein openly challenged the public to try to ride his Rear-Steered Bike I (RSB1). At the time of his co-authored article in *IEEE Control Systems Magazine* [1], the prize money for the first person to successfully ride it was $1,000 US. By the time that the author met Kline for the first time in person, the prize had risen to $5,000 US.

Recognizing the potential difficulty posed by a bicycle that steers in the opposite direction that the handlebars are pointed (i.e. backward brain effect), Klein allowed those seeking conquer the "unridable" bike to choose which configuration from Fig 2 that they wanted for the steer chain.

To successfully complete Klein's challenge, the rider had to remain seated in the saddle, with both feet on the pedals. Furthermore, both wheels had to remain contact with the ground at all times, and the bike needed to make continuous forward progress along the specified path. The path started with a

straight section of 100 ft (30.5 meters) in length, followed by a 90-degree turn, followed by a second 100 ft long straight section. At all times, the bicycle had to remain a distance of 3 ft. (0.9 meters) from the center of the path. When the rider reaches the end of the path, they are to put their feet on the ground, manually turn the bike around, and then ride along the path again, traversing it in the opposite direction.

In an archived web posting [3], Klein stated that over the years, many hundreds of overly optimistic riders attempted to win the prize reward. For some of the most skilled bicyclists and unicyclists, Klein would let them borrow the bike for a month or more to develop their skills. Before fall 2009, there was just one person who was able to remain upright. However, this rider ended up riding haphazardly in an open and flat parking lot as opposed to being able to follow a prescribed path, a necessary condition for winning the prize.

Blame it on the Open Loop Zero

To provide a control theoretic explanation of why Klein's RSB1 is "unridable", Åström, Klein, and Lennartsson [1] derived linearized equations of motion for a simplified bicycle model and constructed transfer functions that relate the lean angle of the bike (output) to the rider torque on the handlebar (input). In an alternate formulation [4], the input is the steering angle δ. They observed that the system has two open loop poles, both real, one negative and the other positive. The two open-loop poles come from the fact that the bicycle behaves like an inverted pendulum, tending to fall toward one side or the other. The transfer function also had an open loop zero. For a bicycle with front wheel steering, the zero was a negative real number, making it fairly straightforward to devise control laws which could stabilize the system.

But in the case of a rear-steered bicycle, the open-loop zero migrates to the right half plane, making it a non-minimum phase system. To make matters worse, for system parameters approximating those of Klein's unridable bike, the open loop zero and open loop pole were in close proximity. An analysis by Åström estimated an upper bound for the phase margin to be about 10^o. This indicates that a rear-steered bicycle, similar to Klein's unridable bike, might be stabilizable in principle. However, such a controller would lack an appropriate level of robustness for a feedback controller that consists of the human brain serving serving as the real-time signal filter, and control law processor, and the human muscles serving as actuators.

For robustness, Åström [4] recommends zero-to-pole ratios that are either less than 0.25 or greater than 4.0. Given that this ratio for the rear-steered bike depends on longitudinal location of center of mass, height of center of mass, and speed, he recommends a strategy of standing tall on the pedals, leaning forward, and pedaling rapidly to get over the $z/p > 4$ threshold as soon as possible. Then, in principle, one could move one's weight back, to sit down, and then "enjoy the ride" once the speed gets sufficiently large [5]. This strategy has been successful on a rear-steered bicycle built at the University of California at Santa Barbara. See also [6]. However, such an approach would violate the rules for Klein's challenge,

Scope of the Current Work

The author became the first person to ride Klein's RSB1, satisfying all the requirements of the challenge. A few weeks later, the author's student, Joe Szalko, became the second. One can think of this article as an exploration of the dynamics and control of rear-steered bikes with the objective of learning how to ride the RSB1 under the conditions specified by Klein's challenge.

The modeling effort is focused on illuminating aspects of bicycle physics that explain what makes riding a rear-steered bicycle different from a bike steered with the front wheel. Here, the paper focuses on the presenting the geometry of steer kinematics and the two types of lateral acceleration that either either have a reinforcing effect or cancelling effect on the lean dynamics of the bike.

Unlike some previous works, the dynamics and control analysis here is performed in the time domain. It considers the natural unstable drift dynamics of the system, and overlays on top of it the control vector field, illuminating the ways that the rider can "push" or "pull" the system through the steering input in order to prevent the bicycle from falling. By expressing the problem in physical terms like forces, accelerations, and velocities, the types of quantities that a rider can feel in the seat of their pants, one can formulate strategies for riding the unridable bike in similar tangible terms.

Klein [12] and Åström et al [1] used the "unridable" rear-steered bicycle as a curious and cautionary case study suitable for engineering students studying dynamic systems and control. In much the same way, this study which takes a deeper exploration into the modeling and control of the system might be a valuable case study for advanced undergraduates and beginning graduate students in engineering.

Bicycle Models

There is a long history of developing mathematical models for bicycles [7]. Depending on how one wants to use the models, some are more appropriate than others. For example, if one wishes to capture the phenomenon of self-stability (i.e. hands-free riding), it would be important to include gyroscopic effects, caster effects, and details of mass distribution [8]. In this study, the goal is to gain insight into what makes RSB1 so difficult to ride, and then use that insight to devise strategies for riding the bike. In this regard, we seek a simple physical model that strips away unimportant effects. We seek a model that a rider can use to interpret what is happening, and to devise a practical strategy for balancing and riding the "unridable" bike.

Inverted Pendulum

A common starting point for modeling a bicycle is a simple one-degree-of-freedom inverted pendulum. The bicycle depicted in Fig 3A consists of a rider fixed rigidly to the bike, whose motion is essentially a side-to-side rotation about a fixed contact point, labeled c, where the tires touch the ground.

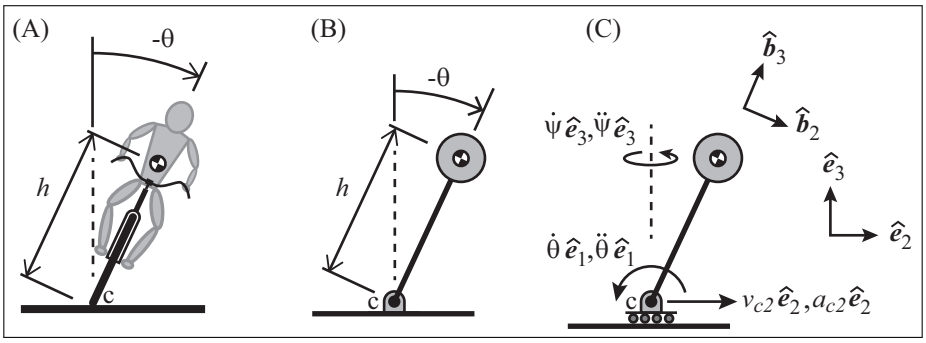

Fig 3. Modeling the lean dynamics of a bicycle as an inverted pendulum.

One of the differences between a bicycle and the common inverted pendulum in Fig 3B, though, is that the rider can move the contact point with the ground laterally. This is depicted in Fig 3C in which the pendulum hinge joint is placed on a roller which can move, $v_{c2}\,\hat{\boldsymbol{e}}_2$, and accelerate, $a_{c2}\,\hat{\boldsymbol{e}}_2$, in the lateral direction.

Anyone who has spent time mastering the skill of balancing an inverted broomstick in the palm of one's hand knows that it can be accomplished by carefully monitoring the lean angle of the pendulum and then quickly, but gracefully, pushing one's hand into the direction of the lean. Likewise, people learning to ride a bike are told to turn the handlebar into the direction of the lean.

The yaw rate also has an influence on the lean angle θ. Here, the yaw rate is the rate of change of the bicycle's heading angle. In Fig 3C, it is depicted as a rotation rate about vertical axis: $\dot{\psi}\,\hat{\boldsymbol{e}}_3$.

A careful derivation of the equations of motion of an inverted pendulum, incorporating the lateral movement and yaw effects described above yields the following:

$$I_{c1}\ddot{\theta} = mgh\sin(\theta) + mh\,a_{c2}\,\cos(\theta) + (I_{c2} - I_{c3})\dot{\psi}^2\cos(\theta)\sin(\theta). \qquad (1)$$

Here, m is the mass of the pendulum, h is the height or distance of the center of mass from the contact point (pendulum pin joint), and g is the gravitational field strength. I_{c1}, I_{c2}, and I_{c3} are moments of inertia about point c corresponding to directions $\hat{\boldsymbol{b}}_1$, $\hat{\boldsymbol{b}}_2$, and $\hat{\boldsymbol{b}}_3$ aligned with principal axes of the bike/rider.

The first term on the right side of (1) is the moment about the contact point c generated by gravity. The second term shows how lateral acceleration affects the lean rate of the pendulum. The final term in (1) captures a destabilizing centripetal effect coming from the yaw rotation.

Steer Kinematics for Front Steered Bike

The primary way that the rider generates a lateral acceleration and a yaw rate is by steering the bike. The mechanical bicycle model used in this study consists of the inverted pendulum described previously attached to a carriage as shown in Fig 4. By modeling the ground contact by a simple carriage, we are intentionally

ignoring the complicated ways that leaned and steered wheels can contact with the ground. The training wheels on the carriage keep the steered wheel and unsteered wheel upright. Furthermore, the steered wheel (front wheel), along with the fork and handlebar, rotate about a vertical "steer axis." This removes caster effects which are not needed to illuminate the differences between front- and rear-steered bicycle dynamics. The carriage provides a simple model of steer kinematics which relates the rider's handlebar steer inputs to the accelerations and rotations that can serve to balance the pendulum.

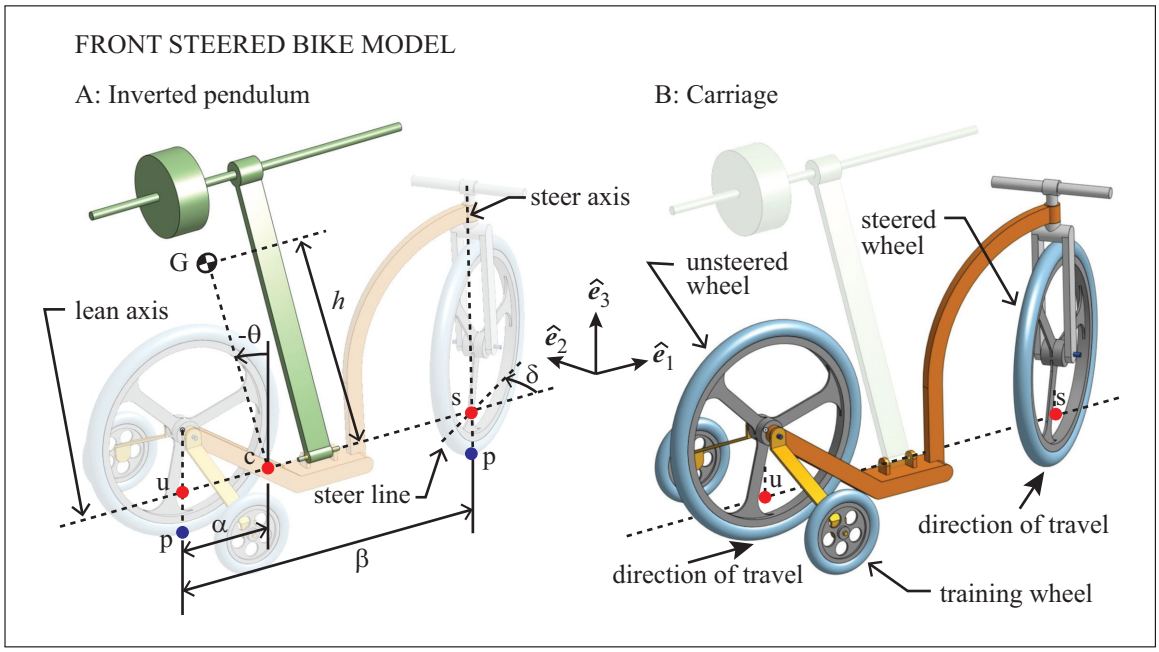

Fig 4. Mechanical model of the front steered bicycle. The model consists of an inverted pendulum attached to a carriage which simplifies the steer kinematics, keeping only the most important effects.

The inverted pendulum is attached to the carriage via a hinge joint. The rotational axis of that hinge joint is labeled "lean axis" in the figure. Three points of particular interest in the kinematics analysis are labeled u, s, and c in Fig 4. All three lie on the lean axis. Point u lies directly below the axle of the rear unsteered wheel and directly above the contact point p with the ground.

Point s is the counterpart for the front (steered) wheel; point s lies at the intersection of the steer axis and the lean axis. Since the steer axis is vertical, point s hovers directly above the point where the steered wheel contacts the ground. In addition to the lean and steer axes, there is a third dashed line in Fig 4A passing through point s called the "steer line." If one were to imagine a vertical plane that sliced the front wheel into a left half and a right half, then this vertical plane would intersect the horizontal plane plane passing through point s along the steer line. The angle between the lean axis and the steer line is δ, the steer angle. The rider gets to choose the steer angle. Generally, δ changes in time.

Finally, point c on the lean axis is aligned with the center of mass of the

pendulum. As the pendulum leans to the left or to the right the center of mass of the pendulum traces out a circular arc that lies in a plane perpendicular to the steer axis. The intersection of this plane with the steer axis is labeled point c. The fact that there are points on Fig 4 and Fig 3 with the same label c is intentional.

Fig 5 shows the a top view of the carriage, along with points u, s, and c as it is executing a left turn. Locations of the rear wheel and front wheel are shaded in light gray so that reader can see geometrically important features. Both Figs. 4 and 5 show mutually perpendicular basis vectors $\hat{\boldsymbol{e}}_1$, $\hat{\boldsymbol{e}}_2$, and $\hat{\boldsymbol{e}}_3$ which define a frame of reference fixed to the frame of the carriage. Unit vector $\hat{\boldsymbol{e}}_1$ is horizontal and tangent to the lean axis; $\hat{\boldsymbol{e}}_2$ is also horizontal. Vector $\hat{\boldsymbol{e}}_3$ is vertical, positive upward.

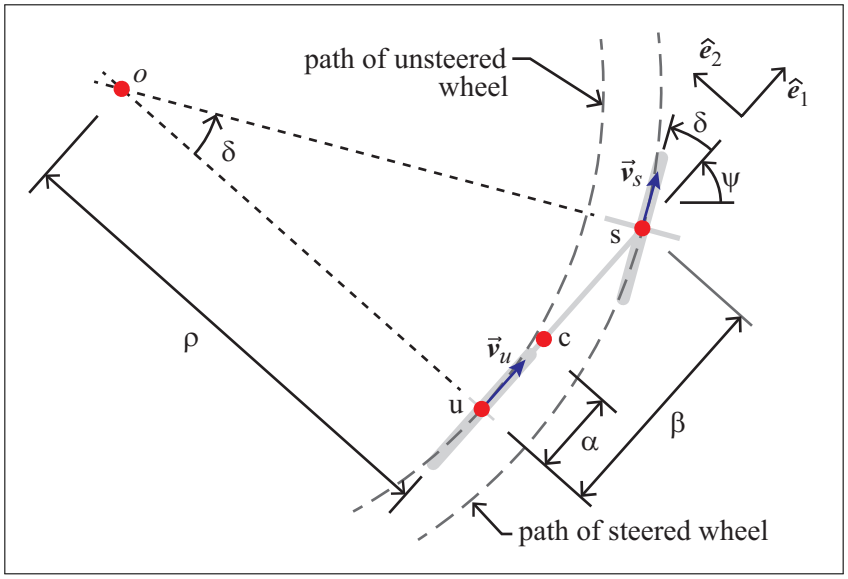

Fig 5. Steer geometry of the front steered carriage.

Since the rear wheel rolls without slipping, point u will move in a direction tangent to the lean axis with velocity

$$\vec{\mathbf{v}}_u = v\,\hat{\boldsymbol{e}}_1. \tag{2}$$

As in the benchmark study of Meijaard et al. [7], this inquiry will consider the case in which the speed v is constant.

If we assume that the front wheel also does not slip, the the velocity of point s, labeled $\vec{\mathbf{v}}_s$ in Fig 5, will always be oriented along the steer line. We can write the velocity of point s as

$$\vec{\mathbf{v}}_s = v_s \cos(\delta)\,\hat{\boldsymbol{e}}_1 + v_s \sin(\delta)\,\hat{\boldsymbol{e}}_2. \tag{3}$$

In general, the speed v_s will be different from v, and it will not be constant.

The yaw rate, discussed previously, is the time derivative of the heading angle ψ defined in Fig 5. Note that since the distance between points u and s does not

change, there is a simple relationship between the velocities of the two points:

$$\vec{\mathbf{v}}_s = \vec{\mathbf{v}}_u + \vec{\mathbf{v}}_{s/u} = v\,\hat{\boldsymbol{e}}_1 + \beta\dot{\psi}\,\hat{\boldsymbol{e}}_2. \tag{4}$$

Here, $\vec{\mathbf{v}}_{s/u}$ denotes the velocity of point s relative to point u, and β is the distance between the points. Reconciling Eqs (4) and (3), one can determine a useful expression for the yaw rate in terms of the steering angle of the carriage:

$$\dot{\psi} = \frac{v\,\tan(\delta)}{\beta}. \tag{5}$$

Recall that the yaw rate affects the lean dynamics (1), at least at quadratic order. More important is its effect on the lateral acceleration of point c.

To write the acceleration of point c, one can express it relative to point u.

$$\begin{aligned}\vec{\boldsymbol{a}}_c &= \vec{\boldsymbol{a}}_u + \vec{\boldsymbol{a}}_{c/u} \\ &= \left(\frac{v^2}{\beta}\tan(\delta)\,\hat{\boldsymbol{e}}_2\right) + \left(-\alpha\dot{\psi}^2\,\hat{\boldsymbol{e}}_1 + \alpha\ddot{\psi}\,\hat{\boldsymbol{e}}_2\right) \\ &= -\alpha\dot{\psi}^2\,\hat{\boldsymbol{e}}_1 + \left(\frac{v^2}{\beta}\tan(\delta) + \alpha\ddot{\psi}\right)\hat{\boldsymbol{e}}_2.\end{aligned} \tag{6}$$

The acceleration $\vec{\boldsymbol{a}}_u$ is rather simple because, at any instant, point u is moving at constant speed along a path with radius of curvature ρ as depicted in Fig 5. In that same figure, it is clear that $\rho = \beta/|\tan(\delta)|$. Similarly, as shown in the second line of (6), it is simple to split $\vec{\boldsymbol{a}}_{c/u}$ into normal and tangential components because points u and c are a fixed distance, α, apart.

The $\hat{\boldsymbol{e}}_2$ component in the final line of Eq (6) is the a_{c2} term in Eq (1). To simplify it a little further, one can take the derivative of (5) and substitute for $\ddot{\psi}$ to get the following expression for the lateral component of acceleration for point c:

$$a_{c2} = \frac{v^2}{\beta}\tan(\delta) + \frac{\alpha\,v}{\beta\,\cos^2(\delta)}\dot{\delta}. \tag{7}$$

This gives us the effective lateral acceleration of the pendulum base in terms of the rider's steer input δ and its derivative $\dot{\delta}$. In upcoming discussions, we will make careful note that the first term scales quadratically in speed v while the second scales linearly.

Steer Kinematics for Rear-Steered Bike

For the rear-steered bicycle, there is a similar pendulum/carriage model as shown in Fig 6. The direction of travel indicated in Fig 6B confirms that the unsteered wheel is at the front of the bike and the steered wheel is at the back. The direction of the $\hat{\boldsymbol{e}}_1$ vector is flipped so that it points in the direction of travel. Also the direction of the steer angle is flipped so that a positive angle δ generates a turn to the left (when facing the direction of travel) just as it did for the front steered bike. Likewise, the lean angle θ for the rear-steered bicycle is defined so that a lean to the left corresponds to a negative value of θ, just as it

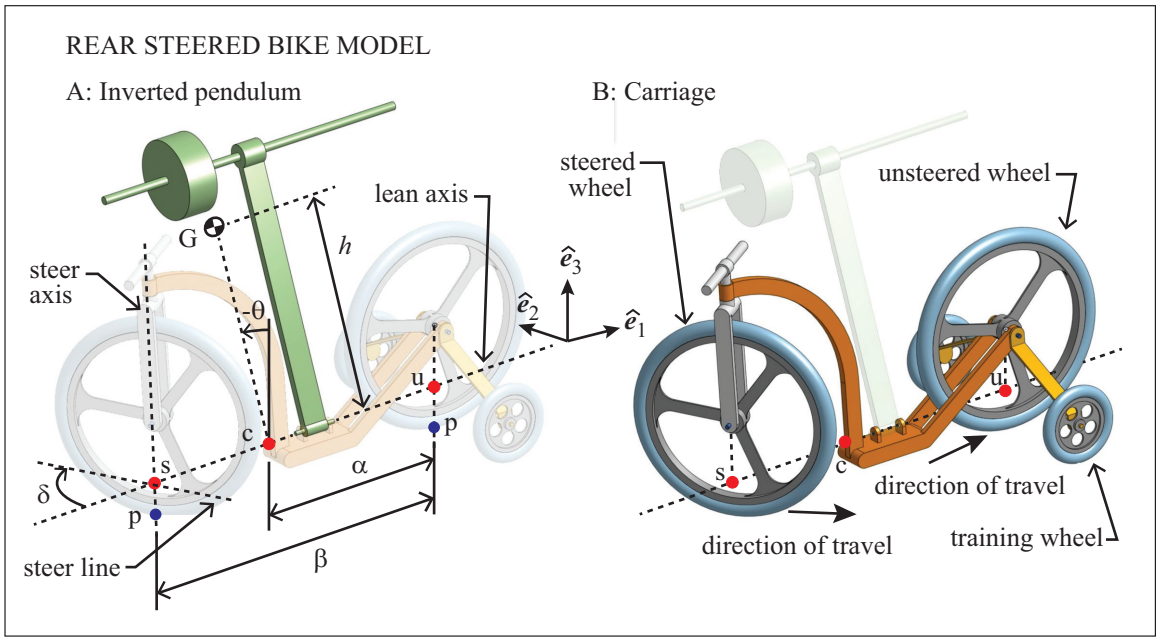

Fig 6. Mechanical model of the rear-steered bicycle.

did for the front steered bicycle. A positive yaw rate still corresponds to a counter-clockwise rotation when viewed from above.

For both RSB1 and a typical front-steered bicycle, the seat is close to the rear wheel. Therefore the center of mass, G, tends to be closer to the rear wheel than the front. Therefore, the value of α, the distance between points c and u is relatively large for the rear-steered bicycle.

The handlebar in Fig 6 is shown attached directly to the fork which turns the steered wheel. It is illustrated this way for simplicity. To depict the chain and sprocket mechanism in the actual rear-steered bike would only complicate the figure since it has no relevance to the steer kinematics.

To work out the steer kinematics of the rear-steered carriage is nearly identical to that of the front steered carriage, but with a few signs flipped. Therefore, there is no need to detail it again. The yaw rate, $\dot{\psi}$, is the same as it was for the front steered carriage (5). The lateral component of acceleration of point c, depending on steer input, is given by

$$a_{c2} = \frac{v^2}{\beta}\tan(\delta) - \frac{\alpha\, v}{\beta\, \cos^2(\delta)}\dot{\delta}. \tag{8}$$

Note that in comparing Eqs (7) and (8) the steer kinematics for the two bike models differ only by the sign of the $\dot{\delta}$ term. That difference gives rise to the positive open loop zero for the rear-steered bike that was mentioned in the introduction.

Linearized Input-Output Equations of Motion

Schwab and Meijjard [9] have reviewed several decades of research in modeling and measuring the ways in which riders control bicycles. It is common for such

studies to think of the rider as the controller element in a closed-loop feedback control system. In many of these models, the rider provides a steer torque to the bicycle handlebar. In others, the rider provides the steer angle instead. The present study adopts a *steer angle* perspective. The goal of the project was for the author to learn how to ride Klein's unridable bike. The choice conforms to the author's view of balancing the bicycle as a process of determining which direction to turn the handlebar and how fast to do it. Furthermore, anyone who has attempted to ride Klein's rear-steered bike knows that it is nearly impossible to develop any appreciable speed. So gyroscopic effects are minimal, as is the rotational inertia about the steer axis. In turning the handlebar, there is little inertia to push against. Therefore, it is rather simple for the rider to generate any reasonable steer rate $\dot{\delta}$ that one desires. In this study, $\dot{\delta}$ is the control input.

As is common, we linearize the system, treating the states θ, $\dot{\theta}$, and δ as small. The result obtained by combining (1), (5), (7) for the front steered bicycle is

$$I_{c1}\ddot{\theta} = mgh\,\theta + mh\left(\frac{v^2}{\beta}\delta + \frac{\alpha v}{\beta}\dot{\delta}\right). \tag{9}$$

For the rear-steered bike, the model equations become

$$I_{c1}\ddot{\theta} = mgh\,\theta + mh\left(\frac{v^2}{\beta}\delta - \frac{\alpha v}{\beta}\dot{\delta}.\right) \tag{10}$$

The terms in parentheses in Eqs. (9,10) are linearized version of the lateral accelerations, a_{c2}.

It is worth noting that if one treats the pendulum as a single point mass, concentrated at a distance h from the lean axis, then (9) is identical to the simplified bike model derived by Timoshenko & Young [10]. It is also equivalent to the first model of Åström et al [1].

In the case of the "benchmark" model, Meijaard et. al [7] meticulously derive linearized equations of motion of the form

$$\begin{bmatrix} M_{\theta\theta} & M_{\theta\delta} \\ M_{\delta\theta} & M_{\delta\delta} \end{bmatrix} \begin{bmatrix} \ddot{\theta} \\ \ddot{\delta} \end{bmatrix} + v \begin{bmatrix} 0 & C_{\theta\delta} \\ C_{\delta\theta} & C_{\delta\delta} \end{bmatrix} \begin{bmatrix} \dot{\theta} \\ \dot{\delta} \end{bmatrix} + \left[g \begin{bmatrix} K_{\theta\theta} & K_{\theta\delta} \\ K_{\delta\theta} & K_{\delta\delta} \end{bmatrix} + v^2 \begin{bmatrix} 0 & \bar{K}_{\theta\delta} \\ 0 & \bar{K}_{\delta\delta} \end{bmatrix} \right] \begin{bmatrix} \theta \\ \delta \end{bmatrix} = \begin{bmatrix} 0 \\ T_\delta \end{bmatrix}. \tag{11}$$

Here, the 13 matrix elements depend on 25 different geometric and mass distribution parameters for the bike, and T_δ is the steer torque. It is of interest to note that if the bicycle has a vertical steer axis which passes through the contact point between the steered wheel and the ground, as in the carriage models of Figs. 4 and 6, then the coefficient $K_{\theta\delta}$ is zero. If, in addition, the centers of mass of the handlebar, fork, and steered wheel all lie on the steer axis, then $M_{\theta\delta}$ is zero also. In this case, the top equation of (11) decouples symbolically from the steer torque T_q. As such, one can write that top equation as

$$M_{\theta\theta}\,\ddot{\theta} = -gK_{\theta\theta}\,\theta - v^2\,K_{\theta\delta}\,\delta - v\,C_{\theta\delta}\,\dot{\delta}. \tag{12}$$

Referring to the "benchmark" model, coefficient $M_{\theta\theta}$ is positive, $C_{\theta\delta}$ is negative, and both $\bar{K}_{\theta\delta}$ and $K_{\theta\delta}$ are negative if you take into account that the sign of the steer angle δ in this study is opposite that of [7]. Therefore Eq. (12) has the same structure and speed dependence as the mathematical model for the front steered bike in (9).

But even if one does not make the assumptions about verticality the steer axis and centers of mass of various parts lining up on that steer axis, the new terms that would appear would be quite small. For example, in the benchmark bike for the benchmark model, the ratio of retained-to-neglected inertia terms is $M_{\theta\theta}/M_{\theta\delta} \approx 35$. The ratio of retained-to-neglected speed-independent "stiffness" terms is $K_{\theta\theta}/K_{\theta\delta} \approx 31$. This is important if one is to use insight gained from studying the simplified model in effort to stabilize and control the real bicycle.

Role of Steer Kinematics in Bike Stabilization

Steer Input

One of the reasons for creating bicycle models with the pendulum separated from the carriage (refer to Figs.4, 6) is to help illuminate a qualitative, physical understanding of what makes the rear-steered bike difficult to ride. This section focuses on a numerical experiment in which both the front steered and rear-steered carriages are traveling so that point u is moving at a constant speed, v. Here, both carriages are given the time-varying steering input defined by the logistic function:

$$\delta(t) = \frac{A}{1 + e^{-kt}}. \tag{13}$$

A plot of δ and its first time derivative, $\dot{\delta}$ appear in Fig 7.

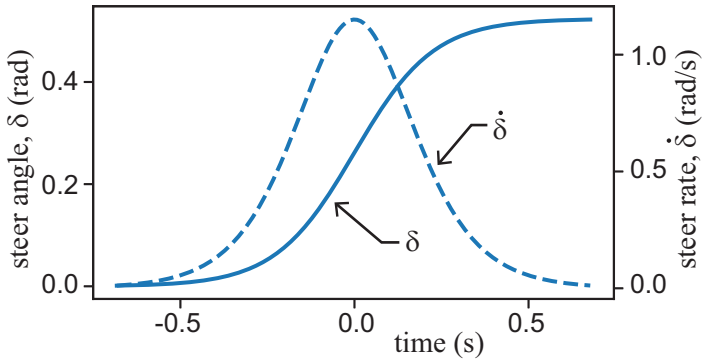

Fig 7. Time dependent steer input δ and its time derivative $\dot{\delta}$ used in the numerical experiment.

Over the time interval shown, the steer angle starts off close to zero, then smoothly but quickly transitions toward another angle $\pi/6 = 30°$, corresponding to a nearly steady left turn. The value of k in (13) was chosen to be $k = 8.79\,\frac{1}{\mathrm{s}}$

so that the 10% to 90% rise time is a half second. If an ordinary, slowly moving bicycle is leaning to the left, a rider might initiate such a steer maneuver in effort to avert a fall.

Wheel Paths

As the front-steered (Fig 4) and rear-steered (Fig 6) carriages execute the steer maneuvers prescribed in Fig 7, the steered and unsteered wheels trace out paths shown in Fig 8. Specifically, the figure shows paths traced out by the points u for the unsteered wheels and points s for the steered wheels that lie on the lean axis.

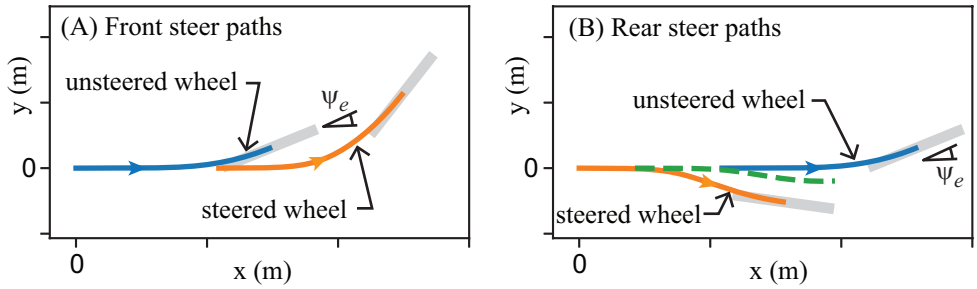

Fig 8. Paths traced out by the two wheels (points u and s) of the carriage as the steer maneuver is executed. (A) Front-steered carriage. (B) Rear-steered carriage. The green dashed curve in (B) shows the path taken by point c, aligned with the center of mass of the pendulum. Plots assumed a speed of $v = 1.1\,\mathrm{m/s}$, and wheel base $\beta = 1.09\,\mathrm{m}$. The plot of point c in panel B corresponds to a center of mass location $\alpha = 0.61\,\beta$, the same as Klein's RSB1. At the final points of the paths shown, two thick gray line segments indicate the locations and orientations of the wheels at that instant.

For the case of the front-steered carriage (Fig 8A), the wheels trace out paths that one might expect. At the beginning, when the steer angle is essentially zero, the two wheels travel along a nearly straight line. But as the handlebar turns the front wheel about the vertical steer axis counter-clockwise when viewed from above, both wheels get pulled *inward* along curves that bend to the left.

The corresponding paths of points u and s for the rear-steered carriage, shown in Fig 8B are qualitatively different. As defined in Fig 6 positive steer angle δ corresponds to a clockwise rotation of the rear wheel about the vertical steer axis when viewed from above. As a consequence, the rear-steered carriage executes a left turn by first swinging the rear wheel *outward* the right.

At the final point for each of the four paths plotted in Fig 8, there is a wide gray segment depicting the positions and orientations of the four wheel of the two carriages at that instant. Observe that for both carriages, the unsteered wheels are at the same heading angle ψ_e at the end of the maneuver, though the carriages took different paths to get there.

Horizontal Acceleration

When it comes to balancing the pendulum, what matters most in the pendulum dynamics (1) is the lateral acceleration of the carriage. Fig 9 shows the acceleration vectors of points u and s for the front-steered carriage along the paths shown in Fig 8A. For the rear, unsteered wheel in Fig 9A, the acceleration is given by

$$\vec{a}_u = \frac{v^2}{\beta} \tan(\delta)\, \hat{\boldsymbol{e}}_2. \tag{14}$$

This is obtained by substituting (5) into (6) and setting $\alpha = 0$. It is a centripetal acceleration with the radius of curvature $\beta/\tan(\delta)$. As such, we see the acceleration vectors pointed inward, toward the center of curvature in Fig 9A.

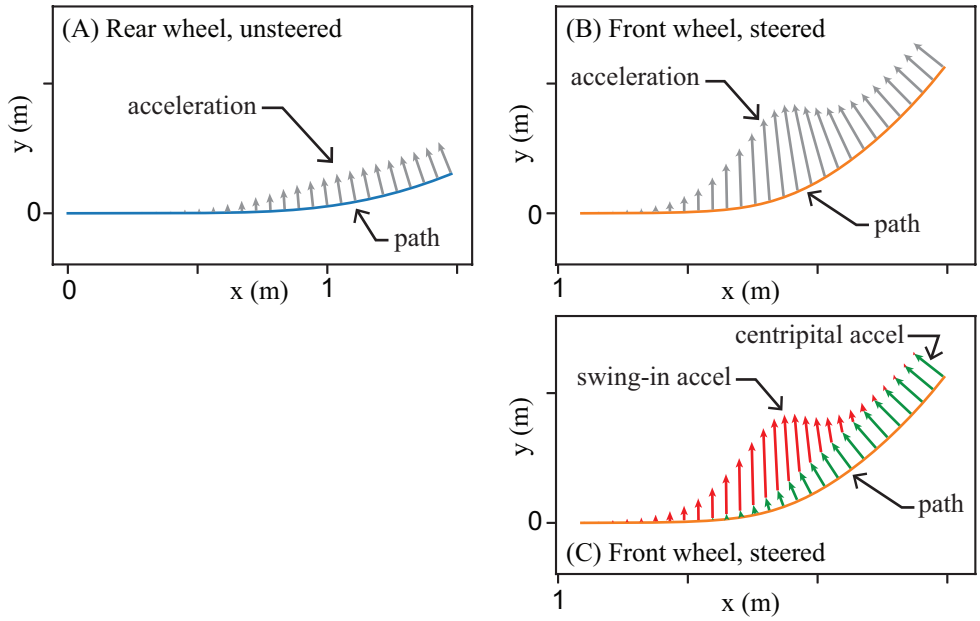

Fig 9. Wheel accelerations of points u and s for the front-steered carriage as it executes the simple steer maneuver. (A) Centripetal acceleration vectors on point u of the rear unsteered wheel. (B) Acceleration vectors on point s of the front wheel are enhanced due to steering action. (C) Two sources of acceleration that enhance each other. Parameters are the same as those listed in Fig 8.

For the front steered wheel, the acceleration contains more terms:

$$\vec{a}_s = \frac{v^2 \tan(\delta)}{\beta}\Big(-\tan(\delta)\, \hat{\boldsymbol{e}}_1 + \hat{\boldsymbol{e}}_2\Big) + \frac{v\dot{\delta}}{\cos^2(\delta)}\, \hat{\boldsymbol{e}}_2. \tag{15}$$

The resulting acceleration vectors of point s on the front-steered carriage appear in Fig 9B. Again, the acceleration vectors point inward along the curved path. Here, one can see that the inward acceleration for the front wheel is even greater than that of the rear wheel of the front-steered bike. This is because the lateral

acceleration in (15) comes from two different sources that reinforce each other. One source of acceleration is a centripetal piece proportional to v^2/β; it is the same as that for the unsteered wheel in (14). The other contribution to the lateral acceleration in (15) is a term proportional to $v\dot{\delta}$. This occurs because turning the front wheel of a front steer bike directs more of the wheel's motion v into the $\hat{\boldsymbol{e}}_2$ direction. We call it the "swing-in" part of the acceleration. These two parts of the acceleration vectors are shown separately in Fig 9C. By placing the vectors tip-to-tail, it is easy to see how the vectors reinforce each other to enhanced the acceleration at point s.

The corresponding plots depicting the acceleration vectors on the rear-steered carriage are presented in Fig 10. As was the case for the front-steered carriage, the unsteered wheel only experiences a simple centripetal acceleration as shown in Fig 10B and points inward.

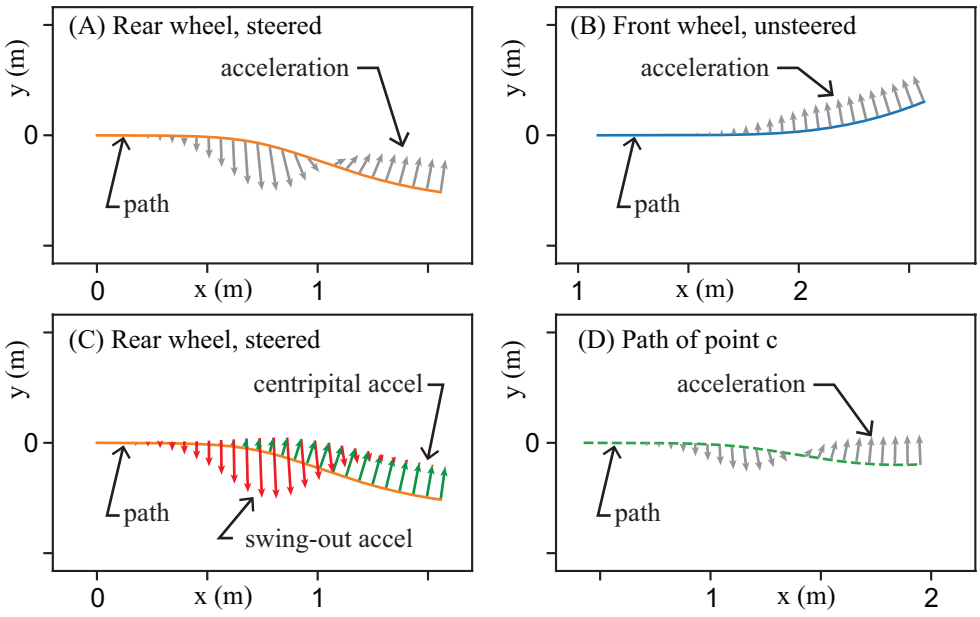

Fig 10. Wheel accelerations of points u and s for the rear-steered carriage as it executes the simple steer maneuver. (A) As the carriage executes a left turn, acceleration vectors of point s of the rear-steered wheel. (B) Acceleration vectors of point u of the front unsteered wheel. (C) Two sources of acceleration that oppose each other on the rear-steered wheel.(D) Acceleration vectors on point c aligned with pendulum center of mass. Parameters are the same as those listed in Fig 8.

As before, the acceleration vectors for the steered wheel come from two different sources: one from a centripetal piece proportional to v^2/β, and another from a piece proportional to $v\dot{\delta}$:

$$\vec{a}_s = \frac{v^2 \tan(\delta)}{\beta}\Big(-\tan(\delta)\,\hat{\boldsymbol{e}}_1 + \hat{\boldsymbol{e}}_2\Big) - \frac{v\dot{\delta}}{\cos^2(\delta)}\,\hat{\boldsymbol{e}}_2. \tag{16}$$

This time, however, the sign of the $v\dot{\delta}$ term is flipped. The resultant acceleration vectors are shown in Fig 10A, and the two parts of steered wheel acceleration are shown in Fig 10C.

The sign change in the $v\dot{\delta}$ portion of the acceleration is due to the fact that the path of the rear-steered wheel swings outward: the steering action of the wheel causes a change in velocity toward the right, even though the bicycle model as a whole turns to the left. For the rear-steered bike, we call it the "swing-out" acceleration.

Fig 10C illustrates how the swing-out acceleration opposes the centripetal acceleration. It is these two opposing components of the acceleration, in contrast to the reinforcing accelerations for the front steered bike, that can make it exceedingly difficult to balance a rear-steered bicycle.

Effect on the Lean Dynamics

What matters for balancing the pendulum of the rear-steered bike model (Fig 6), is the lateral acceleration at point c, the point on the lean axis aligned with the center of mass of pendulum. For Klein's RSB1, the saddle is fixed to the frame near the steer axis of the bicycle. As a result, point c is closer to the steered wheel (point s) than the unsteered wheel (point u) and the lateral acceleration of point c looks more similar to that of point s than point u. Fig 10D shows the acceleration vectors of point c with opposing components similar to that encountered at the steered wheel.

The good news, from the perspective of someone determined to ride Klein's unridable bike, is that these two contributions to the acceleration cannot completely cancel each other. One piece varies with steer angle δ, and the other varies with the derivative, $\dot{\delta}$. Therefore, the two terms are out of phase. The bad news for the prospective rider is that the $\dot{\delta}$ signal leads the δ signal. Therefore, a rider on RSB1 who steers into a lean, as is customary for a traditional bicycle, is going to experience an acceleration that hastens the fall before the centripetal effect kicks in and can (hopefully) avert a crash. It's this dynamic effect of a simple steer maneuver, first causing an outward acceleration and then an inward one, that the rider needs to grapple with in order to balance the bike.

Another aspect one must consider when devising a strategy to ride the rear-steered bike is the role of speed. Recall that the swing-out acceleration is proportional to speed v, while the centripetal acceleration is proportional to v^2. Therefore, the proportion of the two types of opposing accelerations changes as the speed changes.

State Space Analysis

To gain insight into how an aspiring rider might exploit these competing accelerations in effort to stabilize the rear-steered bike, we turn to a state space control perspective. In doing so, we take the linearized mathematical models derived previously (9, 10), and re-write it in standard state space form:

$$\dot{\boldsymbol{x}}(t) = A\,\boldsymbol{x}(t) + \boldsymbol{B}\,u(t), \tag{17}$$

where $\omega = \dot{\theta}$,

$$\boldsymbol{x}(t) = \begin{bmatrix} \theta(t) \\ \omega(t) \\ \delta(t) \end{bmatrix}, \qquad \text{and} \qquad A = \begin{bmatrix} 0 & 1 & 0 \\ \frac{mgh}{I_{c1}} & 0 & \frac{mhv^2}{\beta I_{c1}} \\ 0 & 0 & 0 \end{bmatrix}.$$

The 3×1 B matrices for the for the front steered and rear-steered bicycle models are

$$\boldsymbol{B} = \boldsymbol{B}_f = \begin{bmatrix} 0 \\ \frac{\alpha mhv}{\beta I_{c1}} \\ 1 \end{bmatrix}, \qquad \text{and} \qquad \boldsymbol{B} = \boldsymbol{B}_r = \begin{bmatrix} 0 \\ -\frac{\alpha mhv}{\beta I_{c1}} \\ 1 \end{bmatrix}, \tag{18}$$

respectively. Note that the control input u in (17) represents the steer rate, $\dot{\delta}$. The steer angle δ is included in $\boldsymbol{x}$ and thus is treated as a state.

For the lean dynamics of our simplified bike models, the state space is three dimensional. One can think of the right side of (17) as a vector field. Solutions to the differential equation (17) are integral curves in state space that are everywhere tangent to the vector field.

Drift Dynamics

When we set $u(t) \equiv 0$, we are left with just the natural dynamics of the linearized bike model:

$$\begin{bmatrix} \dot{\theta}(t) \\ \dot{\omega}(t) \\ \dot{\delta}(t) \end{bmatrix} = \begin{bmatrix} 0 & 1 & 0 \\ \frac{mgh}{I_{c1}} & 0 & \frac{mhv^2}{\beta I_{c1}} \\ 0 & 0 & 0 \end{bmatrix} \begin{bmatrix} \theta(t) \\ \omega(t) \\ \delta(t) \end{bmatrix}. \tag{19}$$

One may call this the drift dynamics, and it is the same for both the front-steered and rear-steered bikes.

Since the bottom equation in (19), states that $\dot{\delta} = 0$, the state space of the just the drift dynamics is foliated by invariant planes: $\delta = \text{const}$, as shown in Fig 11. Furthermore, Eq (19) possesses an entire line of equilibria: $(\theta, \omega) = (-\delta v^2/\beta g, 0)$. Thus, for each constant steer angle δ, there is a corresponding equilibrium lean angle θ for which the gravitational moment is exactly balanced by an effective moment due to a constant centripetal acceleration.

Aside from the zero eigenvalue corresponding to the line of equilibria, matrix A in (19) has two other real eigenvalues: $\lambda = \pm\sqrt{mgh/I_{c1}}$, one positive and one negative. Therefore, each equilibrium of the drift dynamics is of saddle type. These are the typical linearized dynamics about the equilibrium of an inverted pendulum. The positive real eigenvalue accounts for the instability corresponding to bike falling to either side. In each $\delta = \text{const}$ invariant plane, the stable and unstable eigenspaces are in directions tangent to eigenvectors $\mathbf{v}_+ = [1 \;\; \sqrt{mgh/I_{c1}} \;\; 0]^T$ and $\mathbf{v}_- = [-1 \;\; \sqrt{mgh/I_{c1}} \;\; 0]^T$, respectively.

Fig 11 shows phase portraits for the saddle equilibria on several different $\delta = \text{const}$ slices. Notice from the v dependence, or lack thereof, in the expressions above, the phase portraits look exactly the same at higher speed, except for the fact that line of equilibria gets more skewed.

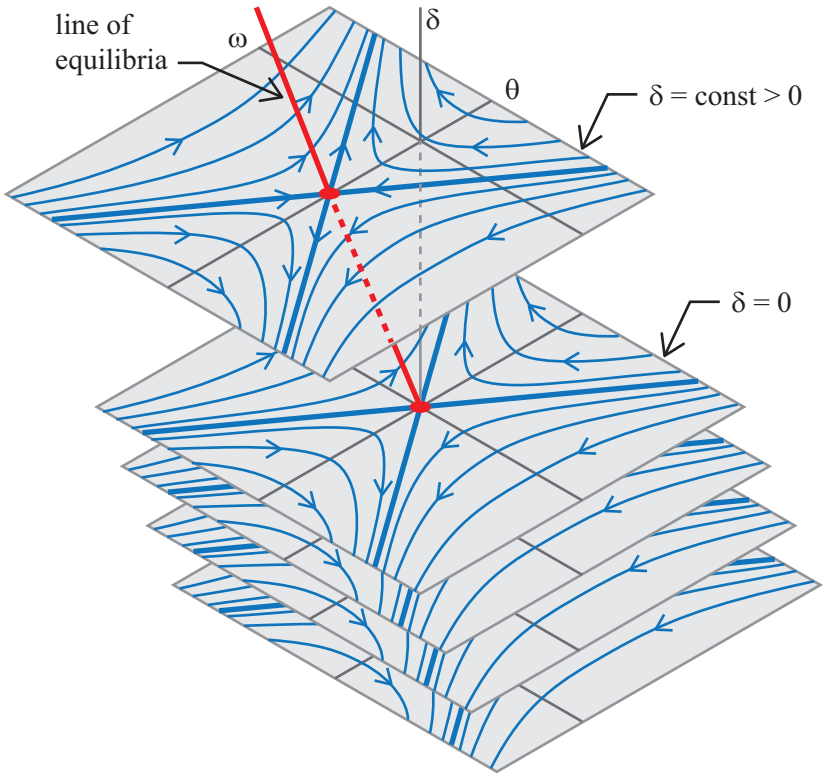

Fig 11. Foliation of phase portraits for the bicycle model's drift dynamics (19)**.**

Adding the Control Vector Field

To more easily visualize the effect of control, on can define a new variable $\tilde{\theta}$ as

$$\tilde{\theta}(t) = \theta(t) + \frac{v^2}{g\beta}\delta. \tag{20}$$

This transformation shifts the line of equilibria to the delta axis, where $(\tilde{\theta}, \omega) = (0, 0)$. As a result, the linearized model with control input, Eq (17), can be re-written as

$$\dot{\tilde{\boldsymbol{x}}}(t) = \tilde{A}\,\tilde{\boldsymbol{x}}(t) + \tilde{\boldsymbol{B}}\,u(t), \tag{21}$$

where

$$\tilde{\boldsymbol{x}}(t) = \begin{bmatrix} \tilde{\theta}(t) \\ \omega(t) \\ \delta(t) \end{bmatrix}, \quad A = \begin{bmatrix} 0 & 1 & 0 \\ \frac{mgh}{I_{c1}} & 0 & 0 \\ 0 & 0 & 0 \end{bmatrix}, \quad \tilde{\boldsymbol{B}}_f = \begin{bmatrix} \frac{v^2}{g\beta} \\ +\frac{\alpha mhv}{\beta I_{c1}} \\ 1 \end{bmatrix}, \quad \tilde{\boldsymbol{B}}_r = \begin{bmatrix} \frac{v^2}{g\beta} \\ -\frac{\alpha mhv}{\beta I_{c1}} \\ 1 \end{bmatrix}. \tag{22}$$

Here, $\tilde{\boldsymbol{B}}_f\,u(t)$ and $\tilde{\boldsymbol{B}}_r\,u(t)$ are the control matrices for the front-steer and rear-steer bike models. Notice that performing this velocity-dependent transformation in (20) removed the v dependence in the drift vector field $\tilde{A}\tilde{\boldsymbol{x}}$. Furthermore, because the new coordinate system is aligned with line of

equilibria, the phase portraits on each leaf of the foliation stack up, as carbon-copies, right on top of each other. Because the right column of $\tilde{A}$ consists of all zeros, there is no steer angle dependence in the new expression of the drift dynamics. One can investigate stability, controllability, and stabilizability by considering only the two dimensional $\tilde{\theta}, \omega$ subspace, where the integral curves of the drift dynamics ($u(t) \equiv 0$) look like those shown in Fig 12A.

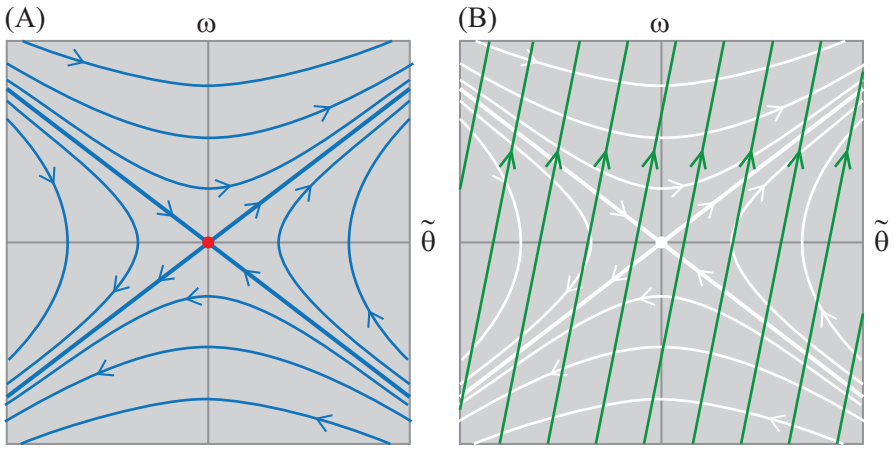

Fig 12. Integral curves for the (A) drift vector field $\tilde{A}\tilde{x}$, and (B) for the control vector field $\tilde{B}u$ when u is a positive constant.

Furthermore, Fig 12B shows integral curves of $\dot{\tilde{x}} = \tilde{\boldsymbol{B}}\, u$, for the control vector field projected onto the $\delta = \text{const}$, $(\tilde{\theta}, \omega)$ subspace. The linearized bicycle model never actually produces solutions like those shown in Fig 12B. However, the curves are useful in that they depict the direction in which the rider can "push" the $(\tilde{\theta}, \omega)$ state of the bike by producing a $\dot{\delta}$ steer input. In this case, the green arrows indicate the direction a rider can "push" the state with a positive *delta*. A negative $\dot{\delta}$ would push in the opposite direction in state space. By overlaying integral curves of the control vector field on top of integral curves of the drift vector field as in Fig 12B, one can see, graphically, what type of steer input would push the state toward the stable eigenspace of the natural drift dynamics.

In the formulation of (21), it is worth noting that all the speed dependence v, appears in the control vector field $\tilde{\boldsymbol{B}}\, u(t)$. The top element of the $\tilde{\boldsymbol{B}}$ matrix is proportional to v^2, corresponding to the centripetal acceleration produced by steer kinematics. The middle element of $\tilde{\boldsymbol{B}}$ is proportional to v, corresponding to the "swing-in" (front-steered bike) or "swing-out" (rear-steered bike) part of the lateral acceleration. And since the two terms depend differently on v, the direction of the control vector field changes for different bike speeds.

Controllability and Stabilizability

Upon constructing the standard controllability matrix $\tilde{R} = [\tilde{\boldsymbol{B}}\ \tilde{A}\tilde{\boldsymbol{B}}\ \tilde{A}^2\tilde{\boldsymbol{B}}]$, one finds that it becomes singular for bicycle speed $v = 0$ and for $v = \alpha\sqrt{mgh/I_{c1}}$. The result holds for both the front-steered and rear-steered bicycles.

It makes sense that controllability is lost for our bike model when $v = 0$. When the bike is not moving, it cannot generate lateral acceleration. More puzzling is that there is a forward speed, well within the range of what would be considered normal cycling speeds, for which the front-steered bike loses controllability.

Front-Steered Bicycle Model

Controllability refers to the property of being able to steer *any* initial state to *any* final state using some combination of the drift vector field and a time-varying control vector field [11]. The control vector field and the drift vector shown in Fig 12 would have a non-singular $\tilde{R}$ corresponding to a controllable system.

In contrast, consider the circumstance shown in Fig 13 depicting what happens to the the state space integral curves when the front-steered bike travel at speed $v = \alpha\sqrt{mgh/I_{c1}}$. Here we see that $\tilde{\boldsymbol{B}}_f$ aligns with the unstable eigenspace of the drift vector field.

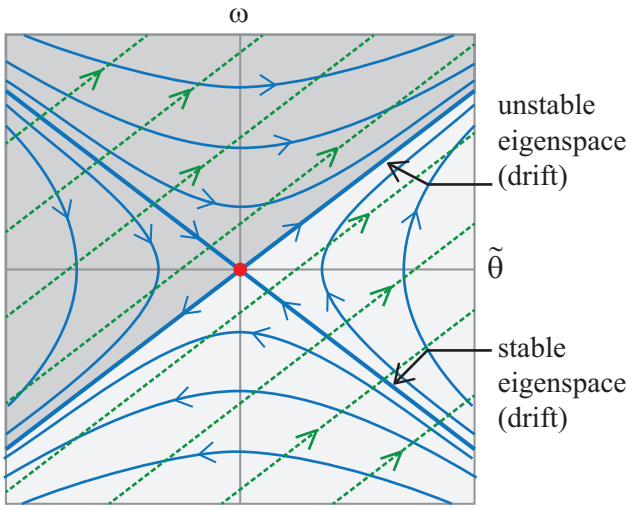

Fig 13. Loss of controllability, from a state space perspective, for the front-steered bike model. Integral curves projected onto a $\delta = \text{const}$ plane for the drift vector field and for the control vector field for the front-steered bike at the speed where the controllability is lost. Integral curves for the drift vector field are solid and shown in blue. Integral curves for the control vector field are dashed and shown in green.

The unstable eigenspace of the drift dynamics shown in the figure is a projection onto a single $\delta = \text{const}$ plane. In the full three dimensional state space of Eq. 21, the unstable eigenspace is a two dimensional, invariant surface that separates the state space into to parts that are indicated by two different shades of gray in Fig 13. In the absence of control, $u = \dot{\delta} = 0$, solutions in the dark gray side, never "drift" to the the light gray side and vice versa. And since

the Control vector field acts tangent to the unstable eigenspace, control action is unable to "push" the dynamic state transversely to the surface. It is impossible use control to steer states on one side of the boundary to the other. Controllability is lost.

To the bicycle rider interested maintaining balance, though, this result is inconsequential. Fig 13 shows that the control vector field does act transverse to the stable eigenspace. To keep the bicycle from falling to one side, the rider can apply a steer input that pushes the state toward the stable eigenspace, then allow the stable component of the drift dynamics carry the state toward the line of equilibria at $(\tilde{\theta}, \omega) = (0, 0)$. Although the linearized model of the front steer bike, loses controllability at one specific speed, it is still *stabilizable* [11] at all forward speeds greater than zero.

Rear-Steered Bicycle Model

Both the front-steered and rear-steered bikes lose controllability at a critical speed we call the *crossover speed*:

$$v = v_{cr} = \alpha\sqrt{mgh/I_{c1}}. \tag{23}$$

In this case, the control vector field lines up with the stable eigenspace as shown in Fig 14A. Therefore, like the loss of controllability for the front-steered bike model, one can use the stable eigenspace to separate state space into a darkly shaded half and a lightly shaded half and argue that, at linear order, the control is unable to push states from one side to the other.

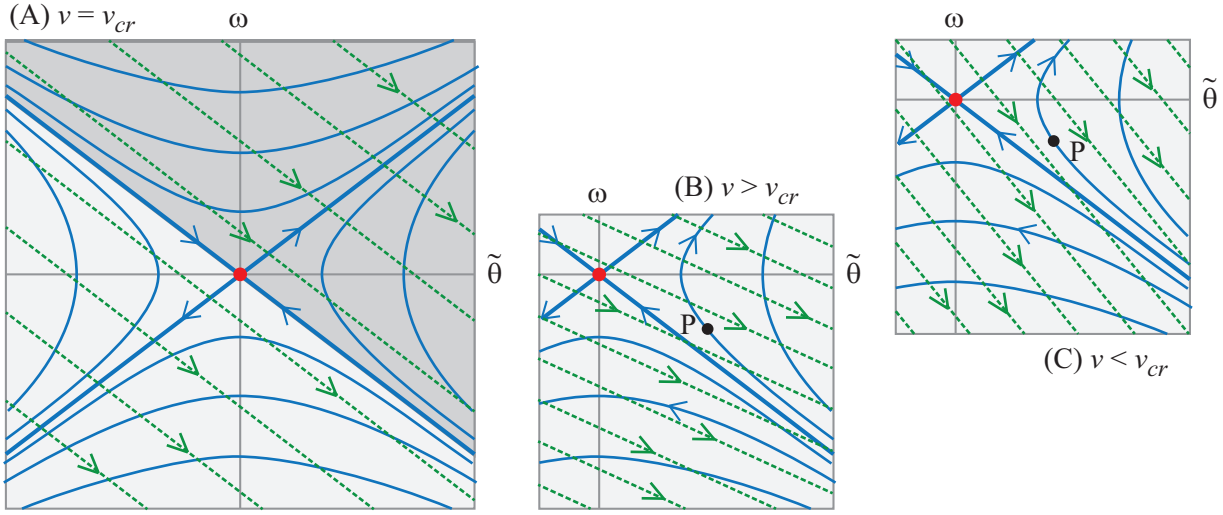

Fig 14. Loss of controllability and crossover for the rear-steered bike model. (A) Integral curves projected onto a $\delta = \text{const}$ plane for the drift vector field and for the control vector field for the rear-steered bike at the speed where the controllability is lost. Integral curves for the drift vector field are solid and shown in blue. Integral curves for the control vector field are dashed and shown in green. (B) Same curves, but for a speed slightly faster than the crossover speed. (C) Same curves, but for a speed slightly slower than the crossover speed.

This time, however, the effect is more pernicious. Since $\tilde{\boldsymbol{B}}_r$ is tangent to the stable eigenspace, it becomes impossible to use control to arrest the unstable dynamics; one cannot steer the state toward the stable eigenspace. Therefore, at the crossover speed $v = v_{cr}$, the rear-steered bike lacks stabilizability too. Connecting this result to the physics of the problem, one can say that loss of stabilizability occurs for the rear-steered bike when the centripetal acceleration (proportional to v^2) and the swing-out acceleration (proportional to v) counteract in a way to make it impossible to actively balance a bike using steer input.

Fig 14B shows overlays of the integral curves of the control vector field on top of integral curves of the drift dynamics. The bike speeds for this case is slightly faster than the crossover speed. Suppose that at some time, the state of the bicycle is at the point labeled P in the figure. Since a positive control input $\dot{\delta}$ creates a "push" in the direction of the green arrows (on the dashed curves) in state space, the rider at state P should choose a sufficiently *negative* steer rate $\dot{\delta} < 0$ to drive the system's dynamics back toward the stable eigenspace.

If one thinks about what this means physically, point P corresponds to the rear-steered bike leaning too far to the right, given the current lean rate ω and steering angle δ. Furthermore, if the rider does not respond to this situation, the bike and rider will fall to the right. As just discussed the portrait in Fig 14B, the appropriate action for the rider to generate a negative steer rate $\dot{\delta}$ which steers the whole bike to the right. This is the normal response for stabilize a leaning bike.

In contrast, look at the overlaid integral curves in Fig 14C where the bike is traveling slightly slower than the crossover speed. Again, one can consider the same state P corresponding to a bike/rider leaning too far to the right. Arrows of the integral curves of the control vector field in this case indicate that the rider should immediately respond with a sufficiently large *positive* steer rate, $\dot{\delta} > 0$. It is important to point out that the control strategy for the rear-steered bike changes on opposite sides of the crossover speed.

For the slower speeds, the swing-out acceleration has a stronger effect than centripetal. Physically, the $\dot{\delta}$ response corresponds to the rider executing a left turn, but doing so in a way that causes the rear, steered wheel to swing to the right to arrest the fall of the right-leaning pendulum.

One final observation to make regarding Figs 14B and C is that when bike speed is close to the crossover speed, the control vector field is mostly aligned with the stable eigenspace. Because of this, it requires a relatively large amount of input to counteract the unstable dynamics.

For the front seer bike, there are no such complications. The control vector field $\tilde{\boldsymbol{B}}_f$ is well aligned with the unstable drift dynamics that one is trying to thwart. The steering strategy is essentially the same regardless of speed.

Strategies for Riding the Rear-Steered Bicycle

It is clear that the ability to stabilize and balance the rear-steered bike model is dependent on the component of vector $\tilde{\boldsymbol{B}}_r$ aligned with the unstable eigenspace

of the uncontrolled drift dynamics. With this in mind, one can decompose $\tilde{\boldsymbol{B}}_r$ into eigen-components:

$$\tilde{\boldsymbol{B}}_r = b_u\,\mathbf{v}_+ + b_s\,\mathbf{v}_- + b_\delta\,\mathbf{v}_0.$$

Here, $\mathbf{v}_+$, $\mathbf{v}_-$, and $\mathbf{v}_0$ are eigenvectors of $\tilde{A}$ corresponding to the positive, negative, and zero eigenvalues. In this case, b_u is given by

$$b_u = \frac{1}{2}\left(\frac{v^2}{g\beta} - \frac{\alpha v}{\beta}\sqrt{\frac{mh}{gI_{c1}}}\right). \tag{24}$$

The quantity b_u is dimensionless and provides a measure of how much authority the rider has, through steering input, to counteract the unstable inverted pendulum dynamics of the bike. The solid curve in Fig 15 is a plot of this "balance authority" as a function of bike speed, v. To generate the plot, numerical values for parameters α and β were measured while the author was sitting on Klein's RSB1. Other parameters h, m, and I_{c1} were based on the benchmark bicycle of Meijaard et al. [7]

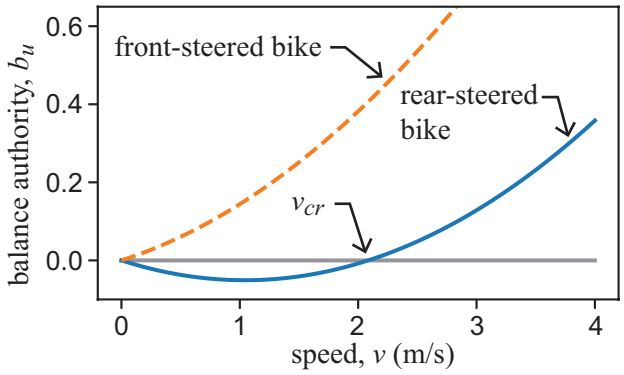

Fig 15. Plot of balance authority, b_u as a function of bike speed, v. The solid curve is b_u given by (24) for the rear-steered bike, while dashed curve is the corresponding measure for a typical front steer bike. Parameters $\beta = 1.09\,\text{m}$ and $\alpha/\beta = 0.61$ were measured from Klein's RSB1, while parameters $m = 94\,\text{kg}$, $h = 0.861\,\text{m}$, $g = 9.81\,\text{N/kg}$, $I_{c1} = 80.8\,\text{kg m}^2$ were obtained from [7]. b_u for the front steer bike is determined by changing the sign of the second term in (24), and using a value of $\alpha/\beta = 0.34$.

The plot shows that for $v = 0$, the balance authority is zero. This is because the control vector $\tilde{\boldsymbol{B}}$ is identically zero at zero speed. With no speed, it is impossible for this particular bike model to turn a steer input into a lateral acceleration that would have an effect on a leaning pendulum.

The control vector, $\tilde{\boldsymbol{B}}$, has parts that are linear and quadratic in speed v, depending on whether they derive from the swing-out or centripetal acceleration effects, In the same way, the expression for b_u in (24) has the same linear and quadratic structure. The value of b_u crosses over from negative to positive at the crossover speed, v_{cr}. The zero value of b_u at the crossover speed corresponds to

loss of the ability to affect the unstable dynamics of the bike, and thus, the loss of stabilizability. The sign flip in b_u corresponds to the input/output behavior of the system switching from that determined by swing-out acceleration to another determined by centripetal acceleration.

For comparison, the analogous balance authority b_u for the front steer bike is also shown in Fig 15 as a dashed curve. This illustrates the profound impact of having the two types of acceleration oppose each other, as they do for the rear-steered bike. The opposition greatly reduces the authority of steer input to balance a rear-steered bike.

Strategy 1: Ride Fast

In [5], Åström suggests a ride-fast strategy for balancing the rear steered bike. By rapidly accelerating past the crossover speed, v_{cr}, this quickly creates separation between the non-minimum phase zero and open-loop unstable pole, allowing for robust stabilization. From the perspective advanced in this article, such an approach would quickly propel the rider into a regime in which the centripetal part of lateral acceleration, proportional to v^2, dominates the swing-out portion, proportional to v. A rider in such a situation would have ample balance authority (Fig 15), and would be able to adopt a balancing strategy of simply turning into the direction of lean, just like a traditional front-steered bicycle.

This strategy actually works for the rear-steered bicycle shown in Fig 16, nicknamed EZRSB (easy rear-steered bike), which is patterned off a similar rear-steered bike that Klein built, which he called "Rear-Steered Bike II." [1, 12] Notice that the seat of the EZRSB bike is relatively far forward, moving the center of mass closer to the front unsteered wheel. This significantly reducing the parameter α. Also, the bike's saddle is relatively high, increasing the rotational inertia, I_{c1}, about the lean axis. Both of these effects tend to lower the crossover speed to approximately 0.4 m/s. This is about 80% lower than that of Klein's "unridable" RSB1, making the threshold much easier to surpass. The corresponding measure of balance authority, b_u, as a function of speed for the EZRSB is provided in Fig 17, with comparisons to a typical front-steered bike and the RSB1.

In the author's experience of riding and observing students ride the EZRSB, if one does not get a strong initial push, it is difficult to pedal fast enough before falling. This is shown in video S2 Video. Compared to the front-steered bike, the balance authority in Fig 17 for the EZRSB is very close to zero over a range of relatively slow speeds. However, if that initial push is sufficient to propel the bike and rider past a certain speed threshold, balancing the Easy Rear-Steered Bike is almost as simple as riding a front-steered bicycle. One cannot ride without hands on the handlebar. But since lateral acceleration of the bike at these higher speeds is dominated by centripetal effects, riding the EZRSB requires no additional rider training, provided that the steer chain is in the figure-8 configuration as shown in Fig 2. In our experience, every rider who has had the fortitude to give the bike a strong enough initial push has been able to succeed at riding it in a controlled manner.

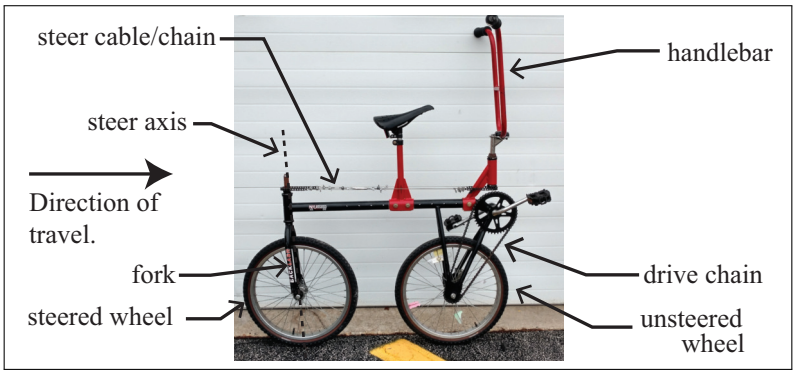

Fig 16. The "Easy Rear-Steered Bicycle" (EZRSB). Built by the author's students. The wheel base is $\beta = 0.62\,\text{m}$; and center of mass location $\alpha = 0.2\,\beta$, leading to a crossover speed of approximately $v_{cr} = 0.4\,\text{m/s}$.

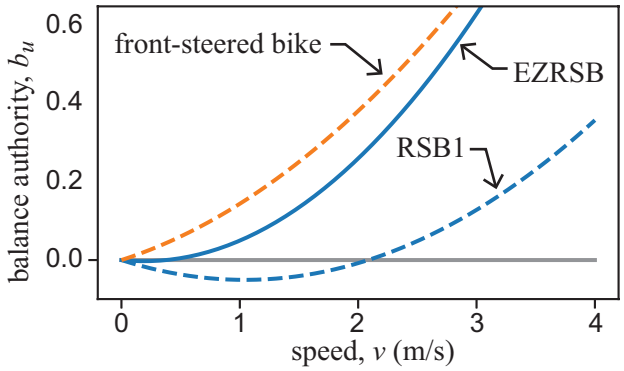

Fig 17. Balance authority for the "Easy Rear-Steered Bicycle" (EZRSB). Comparisons are provided to the same measure on a typical front-steered bicycle (orange dashed), and to Klein's "unridable" RSB1 (blue dashed).

A video of the author riding EZRSB is provided in S3 Video. Although the bicycle itself looks odd, the way that the rider initiates leans, executes turns, and returns the bike to a non-leaned state seem natural. By observing the rotation rate of the wheels, on can estimate the speed of the bike at the beginning of the video at about 2.1 m/s. This is a factor of 5.25 larger than the estimated crossover speed of $v_{cr} = 0.4$ m/s, yielding an open-loop zero to pole ratio of $z/p = 5.25$. This is well past the ratio $z/p = 4$ that Åström [4] recommends for robust control. At this speed, the dimensionless balance authority measure was estimated to be about $b_u = 0.41$.

During experimentation, the author was able to ride the EZRSB as slow as 1.1 m/s, about 2.75 times larger than the crossover speed. We wouldn't expect the bike to get as slow as the crossover speed, where b_u is zero. At a speed of 1.1 m/s, our estimate of the balance authority, according to Eq (24), was approximately $b_u = 0.06$. To be clear, this experimental measure of the author's

ability to balance the EZRSB by first traveling at a high enough speed where it was rather easy to balance the bike, and then slowing down until maintaining balance was no longer possible. S4 Video shows EZRSB operating near this threshold. Accompanying the loss of ability to keep the bike balanced, one also loses directional control.

Another example of a rear-steered bicycle for which the "Ride Fast" strategy works well is a BMX bike trick called the "Fakie", in which riders travel backwards. The interested reader can search on YouTube and find instructional videos that urge riders to keep their weight over the unsteered wheel. Keeping α small reduces the crossover speed.

What has proven to be a good strategy for the EZRSB with its center of mass close to the unsteered wheel (α small), is not a viable approach for Klein's "unridable" Rear-Steered Bike I (RSB1). Because the center of mass on RSB1 is closer to steered wheel (α large), there is a larger "swing out" component of the lateral acceleration. As a consequence, the crossover speed for RSB1 is approximately 2.1 m/s, compared to 0.4 m/s for EZRSB. If achieving a balance authority of $b_u = 0.06$ is imperative for RSB1 as it was for EZRSB, then RSB1 would need an initial push of 2.6 m/s to get it over the threshold where a strategy based on centripetal acceleration would work. If having a zero to pole ratio $z/p = 2.75$ is important, then the initial push on RSB1 would have to produce a speed of 5.8 m/s in less than the fraction of a second that it takes to fall. This is two to five times larger than the initial impulse needed to get the EZRSB going. If one's goal is to satisfy the requirements of Klein's Rear-Steered Bicycle Challenge, then this does not appear to be a viable strategy. The author and his students have not been able to generate a large enough initial speed on RSB1 for which the "Ride Fast" strategy could work.

Strategy 2: Ride Slowly and Swing Out

The relatively high crossover speed for the RSB1 bicycle leads one to explore the possibility of balancing the bike at slow speeds, *below* the crossover. Returning to Fig 15, one can see that low speed control which leverages the "swing-out" acceleration would be a challenge. The lowest speed for which the author was able to ride EZRSB had a balance authority of $b_u = 0.06$. The largest magnitude of b_u that one could experience while traveling slower than the crossover speed is estimated to be $|b_u| = 0.05$. And this occurs at half the crossover speed, giving a pole to zero ratio of $p/z = 2$, about half that recommended by Åström [4] for robustness.

Furthermore, to ride a rear-steered bicycle and keep it balanced at these low speeds, where the swing-out component of acceleration dominates, requires a fundamentally different approach to riding the bike. The physics of the system, combined with the control analysis suggests the following strategy:

1. *Speed control.* The reason why the balance authority curve for RSB1 takes the shape shown in Fig 15 is because of the swing-out acceleration is linearly proportional to speed and the centripetal part of lateral acceleration is quadratic. For the rear-steered bike, these two components

oppose each other, albeit 90° out of phase. The figure shows that balance authority is quite small for all speeds slower than the crossover. But if such an approach is to work, then it would be important for the rider to get into and remain inside a small window of speeds near $\frac{1}{2}v_{cr}$ where the magnitude of b_u is largest.

It is critically important that the rider develop a "feel" for how the bicycle is responding to their control inputs. If the rider recognizes that the bike is not responding sufficient well, the rider should know how to speed up or slow down to improve the outcome.

2. *Exploit the "swing-out."* For low speeds, the lateral component of acceleration that has the strongest impact on lean dynamics is the "swing-out" component. The rider must re-train their brain to recognize that it is not the steer angle δ that is used to balance the bike. Instead, it is the rate at which one turns the handlebar, $\dot{\delta}$, to swing the rear wheel outward, that is important. Again, the rider must develop a productive sense of how it *feels* to swing the rear wheel out in response to lean.

3. *Configure the steer kinematics.* Since the control strategy is to consciously prioritize steering the bicycle's rear end rather than steering the direction of the bike, it is important to configure the steer chain as a simple loop rather than a figure-8 as shown in Fig 2. This way, the rear end of the bike points in the direction of the turned handlebar on RSB1. This is the opposite of what one should choose in the "Ride Fast" strategy.

4. *Direction control.* An important part of Klein's Rear-Steered Bicycle Challenge is to be able to control the direction of the bike. It is not sufficient just to keep it balanced. Klein claimed that at least one rider was able to achieve balance, but "the rider ended up riding haphazardly in an open and flat parking lot as opposed to being able to follow a prescribed path." [3].

   As stated in item 2, the primary means of affecting the lean dynamics of the bike is through $\dot{\delta}$, the rate at which the rider turns the handlebar, not the handlebar angle itself. Once one becomes proficient at keeping the bicycle balanced, one may learn to coordinate the $\dot{delta}$ balance inputs to produce a non-zero average steer angle δ which steers the bike in the desired direction.

Results

The author's students designed and built a rear-steered bicycle similar to Klein's Rear-Steered Bike I. After about a month of training on this rear-steered bike, the author was able to ride it. A few months later, the author coordinated a visit with Richard Klein, and demonstrated that he was able to ride Klein's Rear-Steered Bike I under the conditions specified in the challenge.

Within weeks, one of the author's students, Joe Szalko, also demonstrated that he was able to ride RSB1.

S5 Video shows a video in which the author successfully rides Rear-Steered Bike I (RSB1). This is a typical ride. In comparison to the EZRSB (the "Easy Rear-Steered Bike") of S3 Video, riding RSB1 is a struggle. It demands the rider's complete attention. The rider is consistently providing large steer inputs to keep the bike balanced. And the speed of the bike is slow. This is the nature of riding the previously "unridable" bicycle.

Videos recorded on multiple occasions over several days show that the rider consistently chooses to ride the bike at 1.1 m/s. This consistency suggests that the rider is able to achieve the speed control component (Part 1) of the "Ride Slow" strategy. It is worth noting that the rider's speed of 1.1 m/s almost perfectly matches the bike speed that maximizes the magnitude of balance authority predicted in Fig 15.

Even so, that maximal balance authority at $v \approx \frac{1}{2} v_{cr}$ is still very small. This is why S5 Video shows the rider continually making very rapid steer angle changes. Occasionally one sees steer angle changes of more than 60° or more over a small fraction of a second. The RSB1 rider needs to be constantly vigilant and aggressive.

In the linearized model (10) adopted for the control analysis, there is no limit to the size of the control input u one could apply, or the amount of time one could apply it. Here, in the experiment, one sees that there are limits to how much the rider can actually turn the handlebar. In multiple occasions in the video, the rider is near the limit.

There are occasions in the video in which the rider deviates from item 2 of the "Ride Slow" strategy.These occur when the bike is in a very tight turn. In this case, centripetal acceleration dominates and one can maintain the tight turn by controlling one's speed. It is a different type of bike riding that doesn't appear to have a front-steer counterpart. It is rather fun.

S6 Video shows a rider on RSB1 again, starting at the normal speed of approximately $\frac{1}{2} v_{cr}$. Then the rider increases speed and attempts to ride as fast as possible without losing balance. Repeated measures indicates that this occurs at about 1.6 m/s. This corresponds $b_u = 0.04$ and $p/z = 1.3$ Performing the same experiment, but this time testing how slow the bike can travel without losing the ability to balance and maintain directional control reveals a lower bound on the ridable speed at approximately 0.7 m/s, with $b_u = 0.04$ and $p/z = 3.0$.

Thus, one can conclude that it is possible to ride Klein's Rear-Steered Bike I, maintaining balance and directional control, within a narrow range of slow speeds. Riding the bike within this range requires one to adopt an unconventional strategy that takes advantage of a "swing-out" component of acceleration that depends on the rate at which the rider turns the handlebar. Puzzle solved. Challenge completed.

Conclusion & Reflection

When a five-year-old child learns to ride a bicycle, she does not perform centripetal acceleration calculations, plot wheel trajectories, and then conduct

state space stabilizability analysis. Instead she hops onto the saddle, propels herself forward, falls, gets back up, and tries again, and again, and again. The self-learning neural network inside her brain builds models of how the bike works, and sifts through promising control strategies. In the end, she develops an ability to ride a bike.

There's no reason to believe that a human, with a sufficient amount experience and exploration with the rear-steered bike, couldn't form the appropriate neural connections that would lead to an ability to ride Klein's "Unridable" Bicycle, without ever contemplating a differential equation.

But there is a reason Klein and his collaborators deemed his rear-steered bicycle "unridable." The exploration described here is the first to characterize the difficult to control dynamics physically as a consequence of two types of lateral accelerations that partially cancel each other out. It is the first published study the rear-steered bike as a state-space control problem. The state space perspective illuminates a geometric understanding of what happens to the rear-steered bicycle's dynamics as the speed passes through a "rollover speed" in which the system loses stabilizability. The perspective allows one to develop a measure of balance authority, b_u that appears to provide insight into the conditions for which the bike is and is not ridable.

Most importantly, for this project, the competing accelerations and state space perspective provide insight into how to develop strategies for riding the "unridable" bike. They are strategies that an engineering professor with modest athletic abilities could follow to successfully complete the challenge.

Klein [12] and Åström et al [1] used the "unridable" rear-steered bicycle as a curious and cautionary case study suitable for engineering students studying dynamic systems and control. In much the same way, this study which takes a deeper exploration into the modeling and successful, albeit delicate, control of the system might be a valuable case study for advanced undergraduates and beginning graduate students in engineering.

Supporting Information

S1 Video. Students' attempts to ride Rear-Steered Bike I. Typical attempts to ride a rear-steered bicycle. Attempts appear to be similar regardless of whether the steer chain is configured as a simple loop or figure-8 as depicted in Fig 2. Students in the video are adults and have provided written consent. Link.

S2 Video. Attempt at riding the easy rear-steered bike (EZRSB), but without sufficient initial speed. The author's push off from a lamppost was not sufficient to propel the bike and rider sufficiently past the crossover speed at which the bicycle could be balanced easily. Link.

S3 Video. A successful ride of EZRSB. With sufficient initial speed, the author demonstrates that EZRSB can be balanced with little effort. The end of the video shows that coming to a stop is a different matter. Link.

S4 Video. Riding EZRSB at a slow speed close to balanceability boundary. At a speed of $v = 1.1$ m/s, it becomes difficult for the author to maintain balance and directional control. Link.

S5 Video. Success at riding Klein's "Unridable" Rear-Steered Bike I. Video of the author successfully riding RSB1. Link.

S6 Video. Rear-Steered Bike I traveling (relatively) fast. The bike is ridden at its normal speed close to $\frac{1}{2}v_{cr}$. Then speed is increased until the rider (the author) can no longer balance it. During this, the rider is attempting to travel in a straight line. The precursor to losing balance is a loss of directional control. Link.

Acknowledgment

The author is grateful for his interactions with Professor Richard Klein whose bicycle is the subject of this study. He is also grateful to be able to use Rear-Steered Bike 1 directly in this study.

References

1. Åström KJ, Klein RE, Lennartsson A. Bicycle dynamics and control: adapted bicycles for education and research. IEEE Control Systems Magazine. 2005;25(4):26–47. doi:10.1109/MCS.2005.1499389.
2. SmarterEveryDay. The Backwards Brain Bicycle - Smarter Every Day 133; 2015. Available from: `https://youtu.be/MFzDaBzBlL0?si=H9-JAF_6UhGp8IRT`.
3. Klein R. Bicycle Science - Rear Steer; 2014. Available from: `https://web.archive.org/web/20181209041751/http://www.rainbowtrainers.com/49/`.
4. Åström KJ. Limitations on Control System Performance. European Journal of Control. 2000;6(1):2–20. doi:https://doi.org/10.1016/S0947-3580(00)70906-X.
5. Åström KJ. Bicycle Dynamics and Control; 2004. Available from: `https://citeseerx.ist.psu.edu/document?repid=rep1&type=pdf&doi=97d5f4de8067e5ca2b5186323c598496fd04905d`.
6. Suryanarayanan S, Tomizuka M, Weaver M. System dynamics and control of bicycles at high speeds. In: Proceedings of the American Control Conference; 2002. p. 845–850.
7. Meijaard JP, Papadopoulos JM, Ruina A, Schwab AL. Linearized dynamics equations for the balance and steer of a bicycle: a benchmark

and review. Proceedings of the Royal society A: mathematical, physical and engineering sciences. 2007;463(2084):1955–1982.

8. Kooijman JDG, Meijaard JP, Papadopoulos JM, Ruina A, Schwab AL. A Bicycle Can Be Self-Stable Without Gyroscopic or Caster Effects. Science. 2011;332(6027):339–342. doi:10.1126/science.1201959.

9. Schwab AL, Meijaard JP. A review on bicycle dynamics and rider control. Vehicle System Dynamics. 2013;51(7):1059–1090. doi:10.1080/00423114.2013.793365.

10. Timoshenko S, Young DH. Advanced Dynamics. McGraw-Hill; 1948.

11. Ogata K. Modern Control Engineering. Prentice Hall; 2002.

12. Klein RE. Using bicycles to teach system dynamics. IEEE Control Systems Magazine. 1989;9(3):4–9. doi:10.1109/37.24804.